CHAPTER 4

Results and Discussion

4.1 *Polyalthia evecta* var. *attopeuensis*

The aerial parts of *P. evecta* var. *attopeuensis* were collected from Sakon Nakhon province of Thailand. The air-dried powdered of plant was extracted by percolation with hexane, ethyl acetate and methanol, respectively. Further, the solvents were evaporated to dryness under reduced pressure to afford hexane, EtOAc and MeOH extracts, respectively. The extracts of *P. evecta* var. *attopeuensis* were investigated chemical constituents and biological activities for this research.

4.1.1 Chemical Structure Elucidation of *P. evecta* var. *attopeuensis*

In this investigation, the hexane, ethyl acetate and methanol extracts were carried out for separation, purification, crystallization and structure explanation. Five compounds were mixture of *β*-sitosterol (**173**) and stigmasterol (**178**) from hexane extract, goniothalamin (**211**) from ethyl acetate extract, oxostephanine (**51**) from ethyl acetate and methanol extracts, allantoin (**212**) and dicentrinone (**213**) from methanol extract. The structures have been established on the basis of spectral and physical evidence. It is worth to note that the data from spectroscopic techniques, especially the ^{1}H, ^{13}C-1D and 2D NMR were performed on the accurate molecular structure in Table 4.1–4.9.

1) Mixture of *β*-sitosterol (173) and Stigmasterol (178)

Mixture of compounds **173** and **178** (Fig 4.1) was identified to have molecular formula as $C_{29}H_{50}O$ (414, M^+) and $C_{29}H_{48}O$ (412, M^+). It was isolated from hexane extract as white plates, mp 135.0–136.8 ºC [CH_2Cl_2] (Lit. 134–136 ºC [102]).

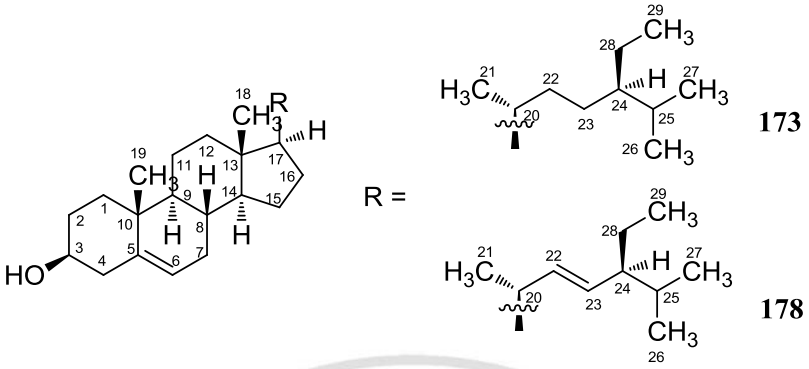

Figure 4.1 The structure of *β*-sitosterol (**173**) and stigmasterol (**178**)

Table 4.1 ^{1}H NMR data of a mixture of *β*-sitosterol (**173**) and stigmasterol (**178**) in comparison with the previously reported [103]

Position	**δ_H (*mult, J* Hz)**		**δ_H (*mult, J* Hz)**	
	Compound 173 and 178 (300 MHz in $CDCl_3$)		**Ref. [103]** (500 MHz in $CDCl_3$)	
	173	**178**	**173**	**178**
3	3.53 (*m*)		3.52 (*m*)	
6	5.36 (*m*)		5.35 (*m*)	
18-CH_3	0.68 (*s*)	0.70 (*s*)	0.68 (*s*)	0.70 (*s*)
19-CH_3	1.01 (*s*)		1.01 (*s*)	
21-CH_3	0.92 (*d*, 6.4)	1.02 (*d*, 6.5)	0.92 (*d*, 6.6)	1.02 (*d*, 6.7)
22	-	5.02 (*dd*, 15.1, 8.7)	-	5.15 (*dd*, 15.2, 8.6)
23	-	5.15 (*dd*, 15.1, 8.6)	-	5.02 (*dd*, 15.2, 8.7)
26-CH_3	0.84 (*d*, 6.5)	0.86 (*d*, 6.8)	0.83 (*d*, 6.5)	0.84 (*d*, 6.5)
27-CH_3	0.81 (*d*, 6.2)	0.80 (*d*, 6.2)	0.81 (*d*, 6.5)	0.80 (*d*, 6.5)
29-CH_3	0.85 (*d*, 7.6)	0.81 (*d*, 7.6)	0.84 (*t*, 7.6)	0.81 (*t*, 7.6)

Remark: δ in ppm from TMS

The ^{1}H NMR spectrum of a mixture of compounds **173** and **178** showed the proton signal for methine proton of H-3 at δ 3.53 (*m*) and represented as the olefinic proton at δ 5.36 (*m*, H-6) of both compounds. The characteristic signals of olefinic proton at δ 5.02 (*dd, J* = 15.1, 8.7 Hz) and δ 5.15 (*dd, J* = 15.1, 8.6 Hz) were assigned to H-22 and H-23 of compound **178**, respectively. The methyl protons at H-18 and H-21 of both compounds were different due to the resonances of **178** were observed more deshield than **173** because of the double bond at C-22. The other proton signals

could not be carried out due to overlapping of the resonances. From evidences and comparison with the previously literature data by Jaitheerapapkul [103], the structures were determined as a mixture of *β*-sitosterol and stigmasterol, see Table 4.1.

The well-known phytosterols biosynthesis, *β*-sitosterol (**173**) and stigmasterol (**178**) has been determined that the isoprene building blocks of the phytosterols via both the mevalonate and deoxyxylulose pathways [104].

2) Goniothalamin (**211**)

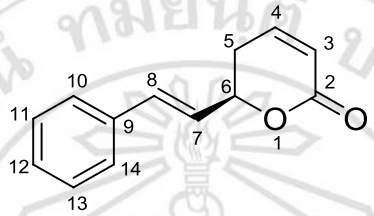

Figure 4.2 The structure of goniothalamin (**211**)

Compound **211** was isolated as white crystals by crystallization from 95% EtOH. It was determined as $C_{13}H_{12}O_2$ (Fig. 4.2) by its EIMS which revealed the molecular ion peak at *m/z* 200 $[M]^+$, mp 80.2–81.3 ºC (Lit. 80.0–82.0 ºC [105]). The UV spectrum (MeOH) showed three bands at 210, 255 and 330 nm which accredited to the aromatic ring with the conjugated bond. The IR absorption showed strong band at 1718 cm^{-1} for C=O stretching and 1243 cm^{-1} for C–O stretching of lactone ring. The medium peaks at 1658, 1505 and 1438 cm^{-1} indicated that C=C stretching of aromatic ring.

The ^1H NMR spectral data are closely to the literature report [105] (Table 4.2). The spectrum exhibited the olefinic proton signals of lactone ring at δ 6.10 (*dt*, *J* = 9.8, 1.7 Hz, H-3) and δ 6.93 (*dt*, *J* = 9.8, 4.3 Hz, H-4). It also showed olefinic protons for H-7 and H-8 at δ 6.28 (*dd*, *J* = 16.0, 6.4 Hz) and δ 6.74 (*d*, *J* = 16.0 Hz), respectively. The methylene proton appeared at δ 2.55 as multiplet signal at H-5. The doublet of doublets at δ 5.11 (*dd*, *J* = 14.2, 6.6 Hz) was assigned to methine proton. Additionally, three signals showed the protons of aromatic ring system at δ 7.34 (*t*, *J* = 7.5 Hz) for H-10 and H-14, δ 7.40 (*d*, *J* = 7.4 Hz) for H-11 and H-13, and δ 7.29 (*d*, *J* = 7.2 Hz) for H-12, respectively.

The ^{13}C NMR and DEPT spectra revealed the down field signal of carbonyl carbon at δ 163.79 (C-2). The methylene carbon signal appeared at δ 29.92 for C-5. The signals of benzene ring were showed at δ 126.71 (C-10 and C-14), δ 128.69 (C-11 and C-13), and δ 128.36 (C-12). Other carbon signals are shown in Table 4.2.

Table 4.2 ^{1}H and ^{13}C NMR data of goniothalamin (**211**) in comparison with the previously reported [105]

Position	Compound 211		Ref. [105]	
	δ_H (*mult, J* Hz) (500 MHz in $CDCl_3$)	δ_C (DEPT) (125 MHz in $CDCl_3$)	δ_H (*mult, J* Hz) (300 MHz in $CDCl_3$)	δ_C (DEPT) (75 MHz in $CDCl_3$)
1	-	-	-	-
2	-	163.79 (C=O)	-	163.5 (C=O)
3	6.10 (1H, *dt*,9.8, 1.7)	121.77 (CH)	6.10 (1H, *dt*,9.8, 1.6)	121.4 (CH)
4	6.93 (1H, *dt*,9.8, 4.3)	144.44 (CH)	6.94 (1H, *dt*,9.8, 4.3)	144.4 (CH)
5	2.55 (2H, *m*)	29.92 (CH_2)	2.57 (2H, *m*)	29.9 (CH_2)
6	5.11 (1H, *dd*,14.2, 6.6)	77.91 (CH)	5.12 (1H, *m*)	77.8 (CH)
7	6.28 (1H, *dd*,16.0, 6.4)	125.70 (CH)	6.92 (1H, *dd*,16.0, 6.3)	125.5 (CH)
8	6.74 (1H, *d*, 16.0)	133.17 (CH)	6.75 (1H, *d*, 16.0)	132.8 (CH)
9	-	135.81 (C)	-	135.5 (C)
10	7.34 (1H, *t*, 7.5)	126.71 (CH)	7.31 (5H, *m*)	126.5 (CH)
11	7.40 (1H, *d*, 7.4)	128.69 (CH)		128.4 (CH)
12	7.29 (1H, *d*, 7.2)	128.36 (CH)		128.1 (CH)
13	7.40 (1H, *d*, 7.4)	128.69 (CH)		128.4 (CH)
14	7.34 (1H, *t*, 7.5)	126.71 (CH)		126.5 (CH)

Remark: δ in ppm from TMS

The assignment of this structure was further proved by 2D NMR analysis (HMQC, HMBC and COSY). The observed correlations are demonstrated in Table 4.3.

Table 4.3 ^{13}C, ^{1}H, HMBC (^{1}H-^{13}C) and COSY (^{1}H-^{1}H) correlations exhibited in the 2D NMR spectra data of goniothalamin (**211**)

Position	**δ_C (DEPT)** (125 MHz in $CDCl_3$)	**δ_H (*mult, J* Hz)** (500 MHz in $CDCl_3$)	**HMBC**	**COSY**
1	-	-	-	-
2	163.79 (C=O)	-	-	-
3	121.77 (CH)	6.10 (1H, *dt*,9.8, 1.7)	C-2, C-5	H-4
4	144.44 (CH)	6.93 (1H, *dt*,9.8, 4.3)	C-2, C-5, C-6	H-3, H-5
5	29.92 (CH_2)	2.55 (2H, *m*)	C-3, C-4, C-6	H-4, H-6
6	77.91 (CH)	5.11 (1H, *dd*,14.2, 6.6)	C-4, C-7, C-8	H-5, H-7
7	125.70 (CH)	6.28 (1H, *dd*,16.0, 6.4)	C-5, C-6, C-9	H-8
8	133.17 (CH)	6.74 (1H, *d*, 16.0)	C-6, C-10	H-7
9	135.81 (C)	-	-	-
10	126.71 (CH)	7.34 (1H, *t*, 7.5)	C-9, C-13	H-11
11	128.69 (CH)	7.40 (1H, *d*, 7.4)	C-8, C-12, C-14	H-10
12	128.36 (CH)	7.29 (1H, *d*, 7.2)	C-10	H-11, H-13
13	128.69 (CH)	7.40 (1H, *d*, 7.4)	C-8, C-12, C-14	H-14
14	126.71 (CH)	7.34 (1H, *t*, 7.5)	C-9, C-13	H-13

Remark: δ in ppm from TMS

The key fragmentation ions in the EIMS was showed by the molecular ion peak at *m/z* 200 $[M]^+$. The ions at *m/z* 103, 97, 90 (base peak) and 77 were useful in getting the structure of **211**. The fragment ion at *m/z* 77 revealed the lose of acetylene from $[C_8H_7]^{\dagger\bullet}$ [106]. The fragmentation patterns are shown in Fig. 4.3.

The styryl lactone, goniothalamin (**211**), is a group of secondary metabolites. It has been purposed via the shikimate pathway [107].

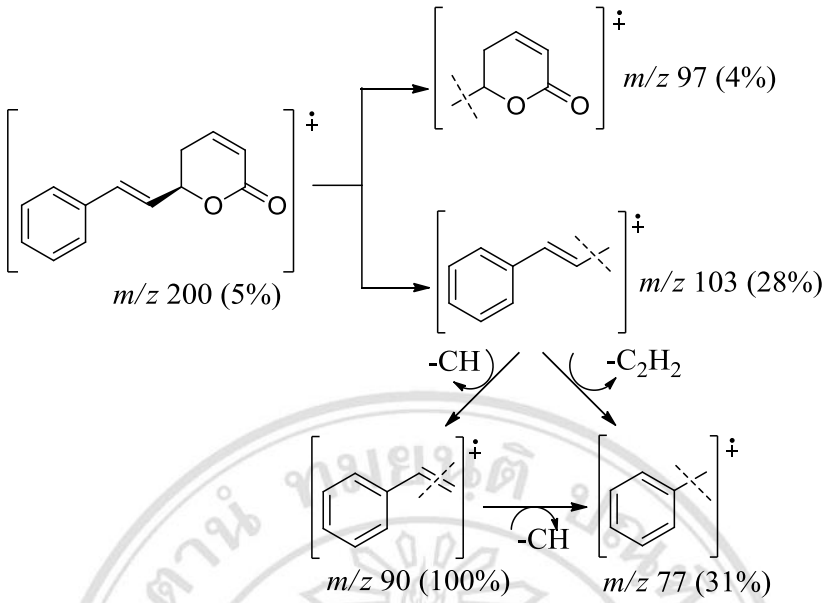

Figure 4.3 The mass spectral fragmentation patterns of goniothalamin (**211**)

3) Oxostephanine (**51**)

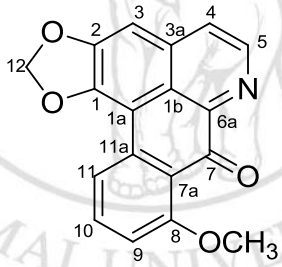

Figure 4.4 The structure of oxostephanine (**51**)

Compound **51** was obtained as yellow needles by crystallization from 95% EtOH, mp 270.0–271.8 ºC (Lit. 270.0–272.0 ºC [108]). The mass spectrum revealed at *m/z* 305 $[M]^+$ corresponding to the molecular formula of $C_{18}H_{11}NO_4$ (Fig. 4.4). The UV absorption bands were observed at λ_{max}^{MeOH} 312 and 272 nm indicating the presence of a conjugated system. The IR absorptions displayed the C=C stretching bands at 1591, 1578 and 1474 cm^{-1} for aromatic ring. The presence of the stretching bands at 1648 cm^{-1} suggested the presence of carbonyl group. The absorptions at 1261 and 1046 cm^{-1} suggested the presence of a C–O–C linkage of ether, at 969 cm^{-1} for methylenedioxy group.

The ^{1}H NMR spectra indicated the presence of methoxyl group at δ 3.98 (*s*, 8-OCH_3). The proton at H-3 of ring A showed a singlet signal at δ 7.08 (*s*) and protons at H-4 and H-5 of ring B appeared as a doublet signal at δ 7.62 (*d*, *J* = 5.2 Hz) and δ 8.76 (*d*, *J* = 5.2 Hz), respectively. The three aromatic protons of ring D were resonated at δ 7.02 (*d*, *J* = 8.4 Hz), δ 7.56 (*t*, *J* = 8.3 Hz) and δ 8.21 (*d*, *J* = 8.1 Hz) for H-9, 10 and 11, respectively. The H-11 has the highest chemical shift due to the deshielding effect caused by forming the hydrogen bonding with the methylenedioxy group. The signal for methylenedioxy was observed at δ 6.27 (*s*, H-12). These spectra agreed with the published data for oxostephanine [109] (Table 4.4).

The ^{13}C NMR and DEPT spectra showed the presence of 18 carbons including one carbonyl, nine quaternaries, six methines, one methylenedioxy and one methoxy carbon. The data are summarized and compared with the literature [109] as shown in Table 4.4.

Further, the structure was analyzed by 2D NMR techniques (COSY, HMQC and HMBC) to confirm the assignments of carbons and protons as the data shown in Table 4.5.

The mass spectrum of compound **51** showed the molecular ion peak at *m/z* 305 $[M]^+$. The ion fragmentations were displayed by EIMS. The base peak was observed at *m/z* 80. The peaks at *m/z* 290 $[M\text{-}CH_3]^+$ and 274 $[M\text{-}OCH_3]^+$ indicated the presence of the methoxy group in ring D [110]. The decarbonylation of aldehydes cleavage at 276 $[M\text{-}CHO]^+$ supported that compound **51** contained one carbonyl group in ring C [111]. Additionally, the presence of methylenedioxy group induced the loss of formaldehyde (CH_2O) and CO [112]. The fragmentation patterns are as shown in Figures 4.5 and 4.6.

The biosynthesis of oxostephanine (**51**) has been determined via the shikimate pathway. The steps of shikimate pathway are summarized by Herrmann [113].

Table 4.4 ^{1}H and ^{13}C NMR data of oxostephanine (**51**) in comparison with the previously reported [109]

Position	Compound 51		Ref. [109]	
	δ_H (*mult, J* Hz) (400 MHz in $CDCl_3$)	δ_C (DEPT) (100 MHz in $CDCl_3$)	δ_H (*mult, J* Hz) (500 MHz in CD_3OD)	δ_C (DEPT) (125 MHz in CD_3OD)
1	-	147.58 (C)	-	147.83 (C)
1a	-	120.88 (C)	-	119.49 (C)
1b	-	122.13 (C)	-	121.61 (C)
2	-	151.71 (C)	-	151.78 (C)
3	7.08 (1H, *s*)	103.11 (CH)	7.13 (1H, *s*)	-
3a	-	146.72 (C)	-	145.25 (C)
4	7.62 (1H, *d*, 5.2)	123.29 (CH)	7.73 (1H, *d*, 5.1)	123.46 (CH)
5	8.76 (1H, *d*, 5.2)	144.84 (CH)	8.65 (1H, *d*, 5.1)	143.28 (CH)
6a	-	135.33 (C)	-	135.27 (C)
7	-	181.74 (C=O)	-	181.16 (C=O)
7a	-	135.23 (C)	-	134.84(C)
8	-	161.91 (C)	-	161.37 (C)
9	7.02 (1H, *d*, 8.4)	112.35 (CH)	7.10 (1H, *d*, 8.5)	111.62 (CH)
10	7.56 (1H, *t*, 8.3)	134.59 (CH)	7.59 (1H, *t*, 8.2)	134.60 (CH)
11	8.21 (1H, *d*, 8.1)	119.74 (CH)	8.17 (1H, *dd*, 8.1, 0.7)	119.36 (CH)
11a	-	108.76 (C)	-	-
12	6.27 (2H, *s*)	102.19 (-OCH_2O-)	6.34 (2H, *s*)	102.28 (-OCH_2O-)
8-OCH_3	3.98 (3H, *s*)	56.44 (-OCH_3)	4.02 (3H, *s*)	55.31 (-OCH_3)

Remark: δ in ppm from TMS

Table 4.5 ^{13}C, ^{1}H, HMBC (^{1}H-^{13}C) and COSY (^{1}H-^{1}H) correlations exhibited in the 2D NMR spectra data of oxostephanine (**51**)

Position	**δ_C (DEPT)** (100 MHz in $CDCl_3$)	**δ_H (*mult, J* Hz)** (400 MHz in $CDCl_3$)	**HMBC**	**COSY**
1	147.58 (C)	-	-	-
1a	120.88 (C)	-	-	-
1b	122.13 (C)	-	-	-
2	151.71 (C)	-	-	-
3	103.11 (CH)	7.08 (1H, *s*)	C-1, C-1b, C-2, C-3	-
3a	146.72 (C)	-	-	-
4	123.29 (CH)	7.62 (1H, *d*, 5.2)	C-1b, C-3	-
5	144.84 (CH)	8.76 (1H, *d*, 5.2)	C-3a, C-4, C-6a	H-4
6a	135.33 (C)	-	-	-
7	181.74 (C=O)	-	-	-
7a	135.23 (C)	-	-	-
8	161.91 (C)	-	-	-
9	112.35 (CH)	7.02 (1H, *d*, 8.4)	C-11	H-10
10	134.59 (CH)	7.56 (1H, *t*, 8.3)	C-7a, C-8	H-9, H-11
11	119.74 (CH)	8.21 (1H, *d*, 8.1)	C-1a, C-9, C-11a	H-10
11a	108.76 (C)	-	-	-
12	102.19 (-OCH_2O-)	6.27 (2H, *s*)	C-1, C-2	-
8-OCH_3	56.44 (-OCH_3)	3.98 (3H, *s*)	C-8	-

Remark: δ in ppm from TMS

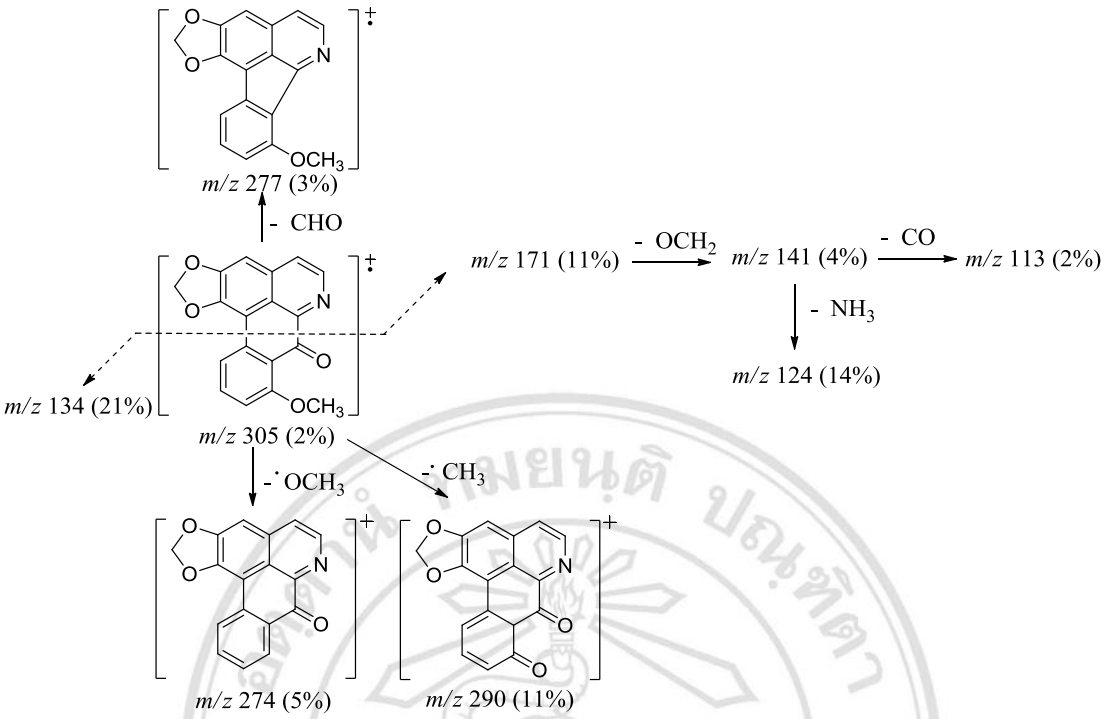

Figure 4.5 The mass spectral fragmentation patterns 1 of oxostephanine (**51**)

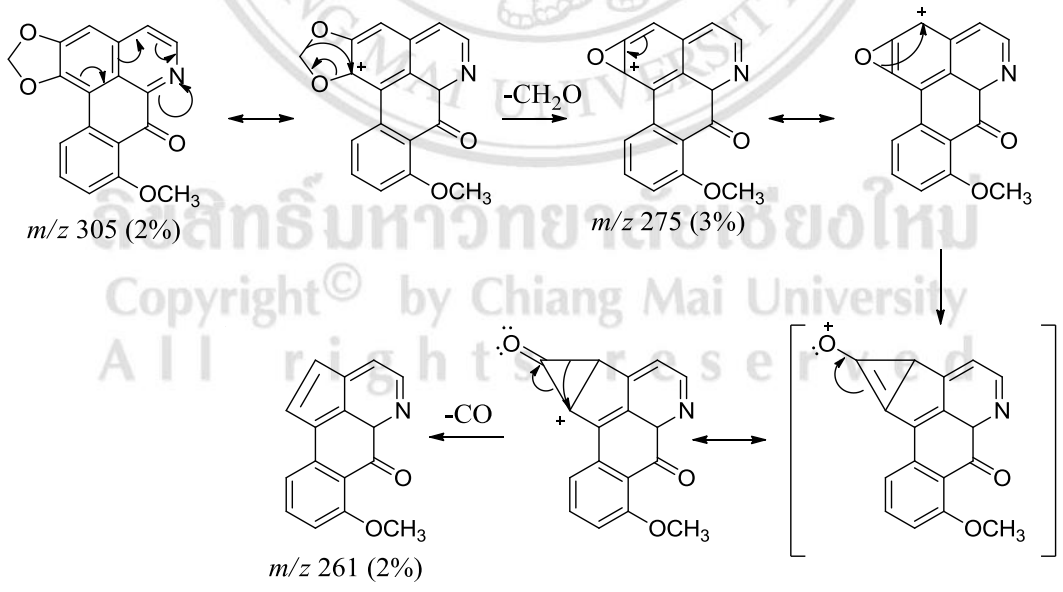

Figure 4.6 The mass spectral fragmentation patterns 2 of oxostephanine (**51**)

4) Allantoin (**212**)

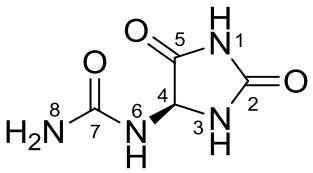

Figure 4.7 The structure of allantoin (**212**)

Compound **212** was obtained as white crystals from recrystallization with MeOH, mp 232.5–234.1 ºC (Lit. 232–235 ºC [114]). The EIMS spectrum revealed the molecular ion $[M]^+$ peak at *m/z* 158 corresponding to the molecular formula of $C_4H_6N_4O_3$. The fragmentation ions peak (Fig. 4.8) at *m/z* 114 corresponding to the cleavage of formamide $[M\text{-}CONH_2]^+$ in this structure [115]. The UV absorptions were observed at λ_{max} 390, 340 and 265 nm in DMSO. The IR spectrum gave a carbonyl group for γ-lactam at 1781 and 1718 cm^{-1}, a carbonyl group for amide at 1655 cm^{-1}. The bands at 3439, 3343 and 3221 cm^{-1} were indicated the presence of N–H group.

The ^1H NMR spectrum showed proton signals of secondary amines of γ-lactam at δ 10.54 (*s*, 1-NH) and δ 8.05 (*s*, 3-NH). The proton of position 6-NH appeared as a doublet at δ 6.88 (*d*, *J* = 8.2 Hz) and position 8-NH_2 assigned as proton of amide at δ 5.78 (*s*), respectively. The methine proton was showed as doublet signal at δ 6.88 (*d*, *J* = 8.2 Hz) for H-4. The proton NMR data of compound **212** was compared with the previously reported [114] as shown in Table 4.6.

The ^{13}C NMR and the DEPT spectral data of **212** revealed four carbon signals consist of three quaternary carbons and one methine carbon as shown in Table 4.6, compare to the previously literature data [114].

The assignments of the chemical shifts in the ^1H and ^{13}C NMR spectra could be made by making use of the correlations observed in the COSY, HMQC and HMBC experiments (see Table 4.7).

Table 4.6 ^{1}H and ^{13}C NMR data of allantoin (**212**) in comparison with the previously reported [114]

Position	Compound 212		Ref. [114]	
	δ_H (*mult, J* Hz) (500 MHz in DMSO-d_6)	δ_C (DEPT) (125 MHz in DMSO-d_6)	δ_H (*mult, J* Hz) (600 MHz in DMSO-d_6)	δ_C (DEPT) (150 MHz in DMSO-d_6)
1	10.54 (1H, *s*)	-	10.54 (1H, *s*)	-
2	-	156.80 (C)	-	156.6 (C)
3	8.05 (1H, *s*)	-	8.04 (1H, *s*)	-
4	5.23 (1H, *d*, 8.2)	62.44 (CH)	5.24 (1H, *d*, 8.2)	62.6 (CH)
5	-	173.63 (C)	-	173.4 (C)
6	6.88 (1H, *d*, 8.2)	-	6.89 (1H, *d*, 8.2)	-
7	-	157.39 (C)	-	157.2 (C)
8	5.78 (2H, *s*)	-	5.78 (2H, *s*)	-

Remark: δ in ppm from TMS

Table 4.7 ^{13}C, ^{1}H, HMBC (^{1}H-^{13}C) and COSY (^{1}H-^{1}H) correlations exhibited in the 2D NMR spectra data of allantoin (**212**)

Position	δ_C (DEPT) (125 MHz in DMSO-d_6)	δ_H (*mult, J* Hz) (500 MHz in DMSO-d_6)	HMBC	COSY
1	-	10.54 (1H, *s*)	C-2, C-5	-
2	156.80 (C)	-	-	-
3	-	8.05 (1H, *s*)	C-2, C-4, C-5	H-4
4	62.44 (CH)	5.23 (1H, *d*, 8.2)	C-5, C-7	H-3, H-6
5	173.63 (C)	-	-	-
6	-	6.88 (1H, *d*, 8.2)	C-4, C-5, C-7	H-4
7	157.39 (C)	-	-	-
8	-	5.78 (2H, *s*)	C-4	-

Remark: δ in ppm from TMS

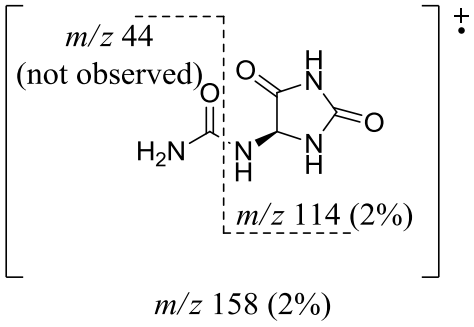

Figure 4.8 The mass spectral fragmentation patterns of allantoin (**212**)

The biosynthesis of allantoin (**212**), there was reported that in plant allantoin might be derived from glyoxylic acid, possibly by condensation with urea which was in basidiomycetes pathway [116].

5) Dicentrinone (**213**)

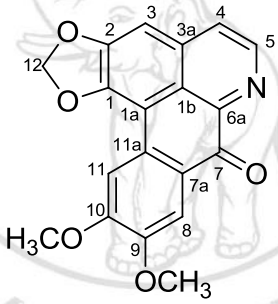

Figure 4.9 The structure of dicentrinone (**213**)

Compound **213** was afforded as orange needles from MeOH:CH_2Cl_2 (80:20), mp 300.0–300.2 ºC (Lit. 300.0 ºC [117]. Its molecular formula was established as $C_{19}H_{13}NO_5$ (Fig. 4.9) by EIMS (*m/z* 335, $[M]^+$). The UV spectrum in MeOH revealed absorption maxima at λ_{max} 344 and 271 nm, indicating the presence of a conjugated system for this structure. The IR showed major absorption bands at 1599, 1564 and 1488 cm^{-1} (C=C stretching of aromatic ring), 1650 cm^{-1} (C=O stretching of carbonyl group), 1262 cm^{-1} (C–O stretching of ether), and 984 cm^{-1} (C–O stretching of methylenedioxy group).

The ^1H NMR spectra showed singlet signal was observed at δ 7.11 (*s*) ascribed to H-3. The doublet proton signals at δ 7.73 (*d*, *J* = 5.2 Hz) and δ 8.87 (*d*, *J* =

5.2 Hz), corresponding to H-4 and H-5 *ortho*-coupling pattern, respectively. The one methylenedioxy group was observed at δ 6.36 (*s*) attributed to H-12. The two aromatic protons of ring D were resonated at δ 7.95 (*s*) and δ 7.96 (*s*) for H-8 and H-11, respectively. Two methoxyl signals appeared as singlet at δ 3.99 (*s*) for 9-OCH_3 and δ 4.08 (*s*) for 10-OCH_3. The spectrum data agreed with the published data for dicentrinone [118] in Table 4.8.

The ^{13}C NMR and DEPT spectra displayed the presence of 19 carbons signals including one carbonyl, ten quaternaries, five methines, one methylenedioxy and two methoxy carbon. The data are summarized in Table 4.8 which compared with the previously reported in the literature [118].

The structure was further confirmed by 2D NMR techniques (COSY, HMQC and HMBC) which showed in Table 4.9.

The mass spectrum of compound **213** showed the molecular ion peak by EIMS at *m/z* 335 $[M]^+$. The base peak was observed at *m/z* 69. The peaks at *m/z* 320, 305 $[M\text{-}CH_3]^+$ and 304, 273 $[M\text{-}OCH_3]^+$ indicated the presence of two methoxy group in ring D [110]. The decarbonylation of aldehydes cleavage at 307 $[M\text{-}CHO]^+$ supported that compound **213** contained one carbonyl group in ring C [111]. Additionally, the presence of methylenedioxy group induced the loss of formaldehyde (CH_2O) and CO [112]. The fragmentation patterns of compound **213** are closely similar to oxostephanine (**51**) because they were the oxoaporphine alkaloids. The mass spectral fragmentation are as shown in Figure 4.10 and 4.11.

The biosynthesis of dicentrinone (**213**) has been determined via the shikimate pathway. The steps of shikimate pathway are summarized by Herrmann [113].

Table 4.8 ^{1}H and ^{13}C NMR data of dicentrinone (**213**) in comparison with the previously reported [118]

Position	Compound 213		Ref. [118]	
	δ_H (*mult, J* Hz) (500 MHz in $CDCl_3$)	δ_C (DEPT) (125 MHz in $CDCl_3$)	δ_H (*mult, J* Hz) (500 MHz in $CDCl_3$)	δ_C (DEPT) (125 MHz in $CDCl_3$)
1	-	151.55 (C)	-	151.6 (C)
1a	-	108.34 (C)	-	108.3 (C)
1b	-	122.64 (C)	-	122.6 (C)
2	-	147.02 (C)	-	147.0 (C)
3	7.11 (1H, *s*)	102.76 (CH)	7.11 (1H, *s*)	102.7 (CH)
3a	-	135.55 (C)	-	135.6 (C)
4	7.73 (1H, *d*, 5.2)	123.96 (CH)	7.73 (1H, *d*, 5.2)	124.0 (CH)
5	8.87 (1H, *d*, 5.2)	144.79 (CH)	8.87 (1H, *d*, 5.2)	144.8 (CH)
6a	-	145.48 (C)	-	145.5 (C)
7	-	181.23 (C=O)	-	181.2 (C=O)
7a	-	127.75 (C)	-	127.8 (C)
8	7.95 (1H, *s*)	108.85 (CH)	7.95 (1H, *s*)	108.9 (CH)
9	-	149.53 (C)	-	149.5 (C)
10	-	153.87 (C)	-	153.9 (C)
11	7.96 (1H, *s*)	109.61 (CH)	7.96 (1H, *s*)	109.6 (CH)
11a	-	125.93 (C)	-	125.9 (C)
12	6.36 (2H, *s*)	102.37 (-OCH_2O-)	6.36 (2H, *s*)	102.4 (-OCH_2O-)
9-OCH_3	3.99 (3H, *s*)	56.14 (-OCH_3)	3.99 (3H, *s*)	56.1 (-OCH_3)
10-OCH_3	4.08 (3H, *s*)	56.27 (-OCH_3)	4.08 (3H, *s*)	56.3 (-OCH_3)

Remark: δ in ppm from TMS

Table 4.9 ^{13}C, ^{1}H, HMBC (^{1}H-^{13}C) and COSY (^{1}H-^{1}H) correlations exhibited in the 2D NMR spectra data of dicentrinone (**213**)

Position	**δ_C (DEPT)** (125 MHz in $CDCl_3$)	**δ_H (*mult*, *J* Hz)** (500 MHz in $CDCl_3$)	**HMBC**	**COSY**
1	151.55 (C)	-	-	-
1a	108.34 (C)	-	-	-
1b	122.64 (C)	-	-	-
2	147.02 (C)	-	-	-
3	102.76 (CH)	7.11 (1H, *s*)	C-1, C-1b, C-2, C-4	H-4
3a	135.55 (C)	-	-	-
4	123.96 (CH)	7.73 (1H, *d*, 5.2)	C-1b, C-5	H-3
5	144.79 (CH)	8.87 (1H, *d*, 5.2)	C-4	-
6a	145.48 (C)	-	-	-
7	181.23 (C=O)	-	-	-
7a	127.75 (C)	-	-	-
8	108.85 (CH)	7.95 (1H, *s*)	C-1a, C-7a, C-10	-
9	149.53 (C)	-	-	-
10	153.87 (C)	-	-	-
11	109.61 (CH)	7.96 (1H, *s*)	C-7, C-9, C-11a	-
11a	125.93 (C)	-	-	-
12	102.37 (-OCH_2O-)	6.36 (2H, *s*)	C-1, C-2	-
9-OCH_3	56.14 (-OCH_3)	3.99 (3H, *s*)	C-10	-
10-OCH_3	56.27 (-OCH_3)	4.08 (3H, *s*)	C-9	-

Remark: δ in ppm from TMS

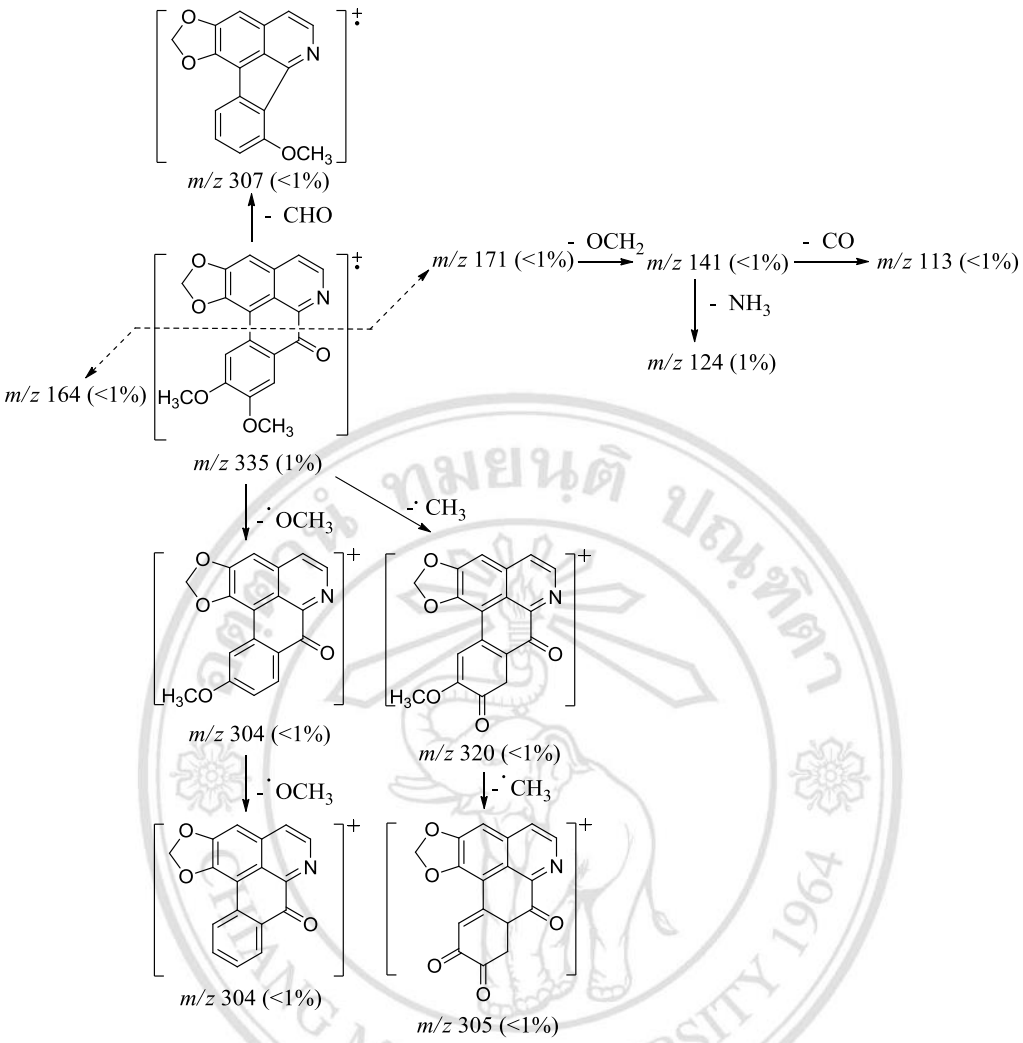

Figure 4.10 The mass spectral fragmentation patterns 1 of dicentrinone (**213**)

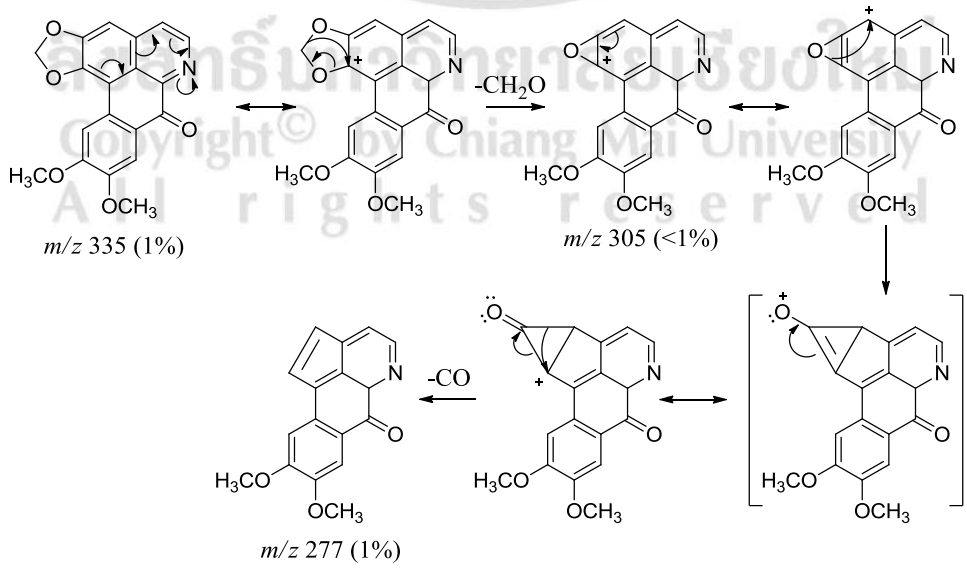

Figure 4.11 The mass spectral fragmentation patterns 2 of dicentrinone (**213**)

4.1.2 Biological Activity of *P. evecta* var. *attopeuensis*

The extracts were submitted for biological evaluation. The preliminary investigations of cytotoxicity testing were carried out by our collaborator from Faculty of Science, Mahidol University. The cytotoxic test were performed on P-388, KB, HT29, MCF-7, A549, ASK and HEK-293 cell lines. The results are summarized in Table 4.10.

Table 4.10 Cytotoxic activities of the extracts from the aerial parts of *P. evecta* var. *attopeuensis*

Extract	ED_{50} (μg/mL)						
	P-388	**KB**	**HT29**	**MCF-7**	**A549**	**ASK**	**HEK-293**
Hexane	10.06	19.47	>20	12.37	>20	>20	12.81
EtOAc	6.11	>20	>20	9.98	>20	19.06	10.76
MeOH	>20	>20	>20	>20	>20	>20	>20
Ellipticine	0.56	0.53	0.61	0.51	0.48	0.49	0.38

ED_{50} <20 μg/mL is considered active
P-388: murine lymphocytic leukemia, KB: human oral epidermoid carcinoma, HT29: human colon carcinoma, MCF-7: human breast cancer, A549: adenocarcinomic human alveolar basal epithelial cells, ASK: rat glioma cell, HEK-293: human embryonic kidney.

The bioassay-guided results from Table 4.10 revealed that the hexane and ethyl acetate extracts showed ED_{50} values lower than 20 μg/mL. The hexane extract exhibited cytotoxicity against P-388, KB, MCF-7 and HEK-293 cell lines with ED_{50} values of 10.06, 19.47, 12.37 and 12.81 μg/mL, respectively. The ethyl acetate extract showed cytotoxicity against P-388, MCF-7, ASK and HEK-293 cell lines with ED_{50} values of 6.11, 9.98, 19.06 and 10.76 μg/mL, respectively. While the methanol extract showed ED_{50} values higher than 20 μg/mL on all cell lines. Due to the limitation of the sample amount, we were unable to get its biological activities of isolated compounds from this plant.

The biological activities of isolated known compounds from *P. evecta* var. *attopeuensis* have been studied and reported as follows.

β-Sitosterol (**173**) and stigmasterol (**178**) are the most prevalent plant sterol. So, these compounds have been evaluated by several biological activities reported, such

as inhibition of DNA polymerase beta lyase activity by deoxyribose phosphate excision assay [119], cytotoxicity against human prostate cancer (PC3 and DU145), human erythroleukemia (K562) and MCF-7 cell lines [120] and antioxidant activity [121].

Goniothalamin (**211**) exhibited cytotoxicity in a variety of cancer cell lines such as cervical (Hela), gastric (HGC-27), ovarian (Caov-3), kidney (786-0), breast carcinomas (MCF-7, T47D and MDA-MB-231), leukemia (HL-60, Jurkat and CEM-SS) [122] and many other types of cancer cell lines [123].

Oxostephanine (**51**), which isolated from *Polyalthia* genus were showed the strongest activity against human lung cancer (SPC-A-1), hepatocellular carcinoma (BEL-7402) cell lines [124], and antibacterial activity against all gram-negative and gram-positive strains tested [89]. Additionally, this compound which isolated from another genus, demonstrated strong activity against cancer cell lines such as acute lymphoblastic leukemia cells (MOLT-3) [125], breast cancer (BC) [125, 126], and KB [126] cell lines.

Allantoin (**212**) was demonstrated weak activities in the both anti-syncytium and anti-human immunodeficiency virus-1 reverse transcriptase (HIV-1 RT) form Polyalthia species [127]. Moreover, this compound has also screen tested anti-bacterial, anti-fungi, anti-herpes simplex virus type-1 (HSV type-1) and anti-parainfluenza type-3 (PI type-3) activities [128].

Dicentrinone (**213**) was evaluated strong cytotoxic against lung (Lu-1) and HEK-293, and moderate against KB, colon (Col-2), MCF-7, ASK and P-388 cancer cell lines, respectivel [129]. Additionally, this compound was also exhibited significant vasorelaxant activity [130], leishmanicidal activity [131] and antiperoxidative activity against the Me linoleate/β-carotene system probably [132].

Therefore, these compounds which isolated from aerial part of *P. evecta* var. *attopeuensis* have gained a significant interest in the anticancer drug development and application for well-being of human in the future.

4.2 *Polyalthia bullata*

4.2.1 Chemical Structure Elucidation of *P. bullata*

1) 5-Hydroxy-3,7,4′-trimethoxyflavone (214)

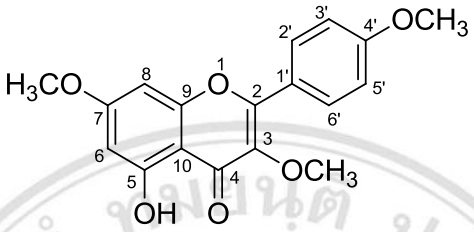

Figure 4.12 The structure of 5-hydroxy-3,7,4′-trimethoxyflavone (**214**)

Compound **214** was purified as yellow crystals [95% EtOH], mp 140.0–140.4 ºC (Lit. 139.0–140.0 ºC [133]). The other name was kaempferol-3,7,4'-*O*-trimethylether. It exhibited a molecular ion peak at *m/z* 328 $[M]^+$ in EIMS, which correspond to the molecular formula $C_{18}H_{16}O_6$. The UV absorptions typical for a flavone were observed at λ_{max} 340 and 288 nm in MeOH. The IR spectrum gave attribute band of C=O stretching of the conjugated carbonyl system at 1637 cm^{-1}, which slightly shift to the lower frequency due to the presence of intramolecular hydrogen bonding. The C=C stretching of aromatic ring appeared at 1616, 1508 and 1496 cm^{-1}. The O-H and C–O stretching bands of phenolic compound were assigned at 3472 and 1257 cm^{-1}, respectively.

The ^{1}H NMR spectrum (Table 4.11) exhibited proton signals for six aromatic protons, consist of two *meta* coupling protons for ring A; δ 6.38 (*d*, *J* = 2.2 Hz, H-6) and δ 6.47 (*d*, *J* = 2.2 Hz, H-8), and four *ortho* coupling protons for ring B; δ 8.10 (*d*, *J* = 9.1 Hz, H-2', 6') and δ 7.05 (*d*, *J* = 9.1 Hz, H-3', 5'), respectively. The resonances of three methoxy groups were appeared as singlets at δ 3.88 (*s*, 3-OCH_3), 3.90 (*s*, 7-OCH_3) and 3.92 (*s*, 4'-OCH_3), respectively. The presence of singlet signal of 5-OH at δ 12.69 supported a chelated hydroxy proton.

Table 4.11 ^{1}H and ^{13}C NMR data of 5-hydroxy-3,7,4′-trimethoxyflavone (**214**) in comparison with the previously reported [133]

Position	Compound 214		Ref. [133]	
	δ_H (*mult, J* Hz) (400 MHz in $CDCl_3$)	δ_C (DEPT) (100 MHz in $CDCl_3$)	δ_H (*mult, J* Hz) (400 MHz in $CDCl_3$)	δ_C (DEPT) (100 MHz in $CDCl_3$)
1	-	-	-	-
2	-	155.97 (C)	-	156.1 (C)
3	-	138.86 (C)	-	139.0 (C)
4	-	178.78 (C=O)	-	179.0 (C=O)
5	-	162.01 (C)	-	161.9 (C)
6	6.38 (*d*, 2.2)	97.82 (CH)	6.34 (*d*, 2.0)	98.0 (CH)
7	-	165.39 (C)	-	165.6 (C)
8	6.47 (*d*, 2.2)	92.16 (CH)	6.43 (*d*, 2.0)	92.3 (CH)
9	-	156.75 (C)	-	156.9 (C)
10	-	106.06 (C)	-	106.2 (C)
1′	-	122.81 (C)	-	123.0 (C)
2′, 6′	8.10 (*d*, 9.1)	130.17 (CH)	8.07 (*d*, 9.0)	130.4 (CH)
3′, 5′	7.05 (*d*, 9.1)	114.06 (CH)	7.01 (*d*, 9.0)	114.3 (CH)
4′	-	161.67 (C)	-	162.2(C)
3-OCH_3	3.88 (*s*)	60.16 (CH_3)	3.86 (*s*)	60.3 (CH_3)
7-OCH_3	3.90 (*s*)	55.80 (CH_3)	3.87 (*s*)	55.9 (CH_3)
4′-OCH_3	3.92 (*s*)	55.44 (CH_3)	3.89 (*s*)	56.0 (CH_3)
5-OH	12.69 (*s*)	-	12.70 (*s*)	-

Remark: δ in ppm from TMS

The ^{13}C NMR and DEPT spectra revealed the presence of one carbonyl carbon, eight quaternary carbons, six methine carbons and three methoxyl carbons as shown in Table 4.11.

This structure were confirmed by comparison of ^{1}H and ^{13}C NMR data with previously reported in Table 4.11 [133] and further identified by 2D NMR techniques (COSY, HMQC and HMBC) as shown in Table 4.12.

Table 4.12 ^{13}C, ^{1}H, HMBC (^{1}H-^{13}C) and COSY (^{1}H-^{1}H) correlations exhibited in the 2D NMR spectra data of 5-hydroxy-3,4′,7-trimethoxyflavone (**214**)

Position	**δ_C (DEPT)** (100 MHz in $CDCl_3$)	**δ_H (*mult*, *J* Hz)** (400 MHz in $CDCl_3$)	**HMBC**	**COSY**
1	-	-	-	-
2	155.97 (C)	-	-	-
3	138.86 (C)	-	-	-
4	178.78 (C=O)	-	-	-
5	162.01 (C)	-	-	-
6	97.82 (CH)	6.38 (*d*, 2.2)	C-5, C-7, C-8, C-10	H-8
7	165.39 (C)	-	-	-
8	92.16 (CH)	6.47 (*d*, 2.2)	C-6, C-7, C-9, C-10	H-6
9	156.75 (C)	-	-	-
10	106.06 (C)	-	-	-
1'	122.81 (C)	-	-	-
2′, 6′	130.17 (CH)	8.10 (*d*, 9.1)	C-2, C-2′, C-4′	H-3′, 5′
3′, 5′	114.06 (CH)	7.05 (*d*, 9.1)	C-1′, C-4′, C-5′	H-2′, 6′
4′	161.67 (C)	-	-	-
3-OCH_3	60.16 (CH_3)	3.88 (*s*)	C-3	-
7-OCH_3	55.80 (CH_3)	3.90 (*s*)	C-7	-
4′-OCH_3	55.44 (CH_3)	3.92 (*s*)	C-4′	-
5-OH	-	12.69 (*s*)	C-5, C-6, C-10	-

Remark: δ in ppm from TMS

The EIMS analysis revealed that a characteristic fragmentation behavior of compound **214** ($[M]^+$, *m/z* 328). The base peak was showed at *m/z* 327 $[M-H]^+$. The main fragments produced by the retro Diels-Alder cleavage of ring C bonds yielded the fragment ions at *m/z* 166 and *m/z* 162, respectively. Further, the loss of methyl group $[M-CH_3]^+$, followed by the loss of dehydration $[M-CH_3-H_2O]^+$ and carbonyl group $[M-CH_3-H_2O-CO]^+$. Compound **214** exhibited the fragment ions like in the case of fragmentation patterns of other flavones, which observed by the previously published [134] as shown in Figure 4.13.

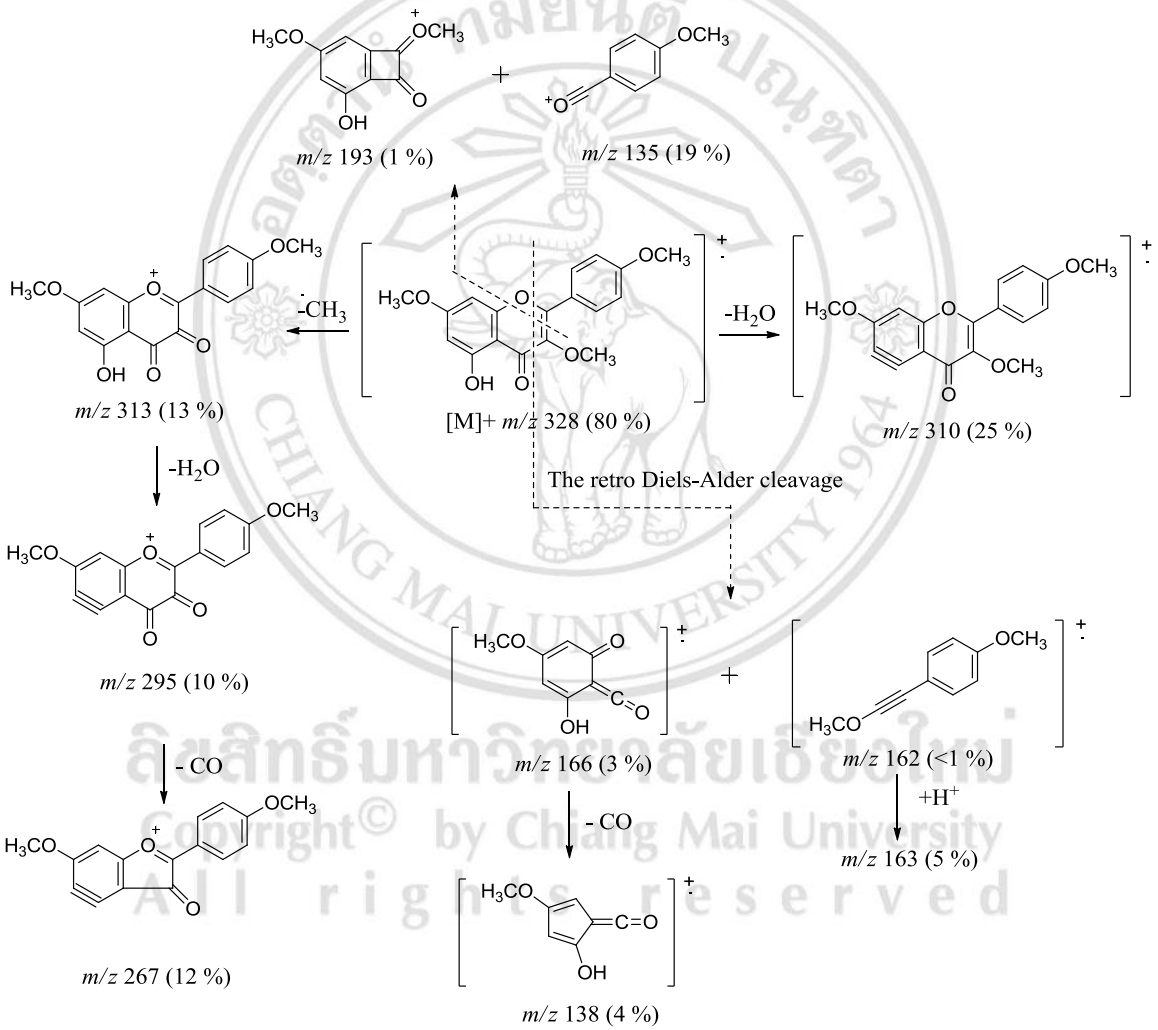

Figure 4.13 The mass spectral fragmentation patterns of 5-hydroxy-3,4′,7-trimethoxyflavone (**214**)

2) 5,3′-Dihydroxy-3,7,4′-trimethoxyflavone (215)

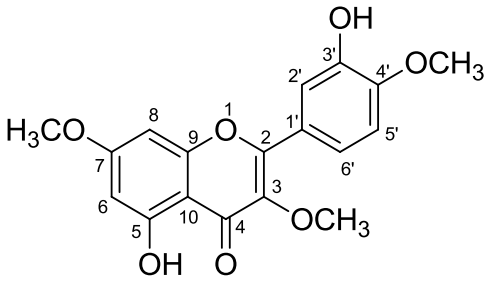

Figure 4.14 The structure of 5,3′-dihydroxy-3,7,4′-trimethoxyflavone (**215**)

Compound **215** was recrystallized with mixtures of 95% EtOH, MeOH and CH_2Cl_2 to obtain as yellow needles. The other names were 3,7,4'-*O*-trimethylquercetin or commonly called ayanin. The mass spectrum gave a molecular ion peak at m/z 344 $[M]^+$ which correspond to the molecular formula $C_{18}H_{16}O_7$, mp 172.5–173.0 ºC (Lit. 169.0–171.0 ºC [135]). The UV absorptions of flavone skeleton at λ_{max} 356, 255 and 207 nm in MeOH. The IR spectrum showed C=O stretching at 1657 cm^{-1} for the conjugated carbonyl system in ring C. The C=C stretching bands of aromatic ring exhibited at 1590 and 1500 cm^{-1}. The O–H and C–O stretching bands of phenolic compound were assigned at 3480 and 1220 cm^{-1}, respectively.

The ^1H NMR spectrum (Table 4.13) revealed two proton signals which occurred as *meta*-coupled doublets at δ 6.38 (*d, J* = 2.2 Hz, H-6) and δ 6.47 (*d, J* = 2.2 Hz, H-8). The other aromatic protons exhibited at δ 7.72 (*d, J* = 2.2 Hz), 6.99 (*d, J* = 8.6 Hz) and 7.75 (*dd, J* = 8.6, 2.2 Hz) assigned to H-2', H-5' and H-6', respectively. The signals of three methoxy groups were appeared singlets at δ 3.89 (*s*, 3-OCH_3), 3.90 (*s*, 7-OCH_3) and 4.01 (*s*, 4'-OCH_3), respectively. The low field singlet signal at δ 12.66 (*s*) indicated the presence of a chelated hydroxy proton for 5-OH and another hydroxyl group at δ 5.76 (*s*) was assigned to 3'-OH.

The ^{13}C NMR and DEPT spectrum indicated the presence of 18 carbons that were one carbonyl carbon, nine quarternary carbons, five methine carbons and three methoxyl carbons as shown in Table 4.13.

These spectral data were compared with the literature values [135, 136], as can be seen in Table 4.13, and then confirmed structure by 2D NMR techniques (COSY, HMQC and HMBC) as shown in Table 4.14.

Table 4.13 ^{1}H and ^{13}C NMR data of 5,3′-dihydroxy-3,7,4′-trimethoxyflavone (**215**) in comparison with the previously reported [135]

Position	Compound 215		Ref. [135]	
	δ_H (*mult, J* Hz) (400 MHz in $CDCl_3$)	δ_C (DEPT) (100 MHz in $CDCl_3$)	δ_H (*mult, J* Hz) (400 MHz in $CDCl_3$)	δ_C (DEPT) (100 MHz in $CDCl_3$)
1	-	-	-	-
2	-	155.67 (C)	-	148.1 (C)
3	-	139.14 (C)	-	140.4 (C)
4	-	178.82 (C=O)	-	180.3 (C=O)
5	-	161.96 (C)	-	158.4 (C)
6	6.38 (*d*, 2.2)	97.87 (CH)	6.35 (*d*, 2.0)	99.2 (CH)
7	-	165.44 (C)	-	167.3 (C)
8	6.47 (*d*, 2.2)	92.12 (CH)	6.46 (*d*, 2.0)	93.5 (CH)
9	-	156.74 (C)	-	163.5 (C)
10	-	106.10 (C)	-	107.3 (C)
1′	-	123.62 (C)	-	124.8 (C)
2′	7.72 (*d*, 2.2)	114.39 (CH)	7.68-7.70 (*m*)	116.5 (CH)
3′	-	145.50 (C)	-	151.6 (C)
4′	-	148.63 (C)	-	157.4 (C)
5′	6.99 (*d*, 8.6)	110.36 (CH)	6.96 (*d*, 8.8)	112.6 (CH)
6′	7.75 (*dd*, 8.6, 2.2)	121.58 (CH)	7.68-7.70 (*m*)	122.6 (CH)
3-OCH_3	3.89 (*s*)	60.16 (CH_3)	3.88 (*s*)	60.9 (CH_3)
7-OCH_3	3.90 (*s*)	55.80 (CH_3)	3.99 (*s*)	57.0 (CH_3)
3′-OH	5.76 (*s*)	-	5.68 (*s*)	-
4′-OCH_3	4.01 (*s*)	56.05 (CH_3)	3.88 (*s*)	57.1 (CH_3)
5-OH	12.66 (*s*)	-	12.63 (*s*)	-

Remark: δ in ppm from TMS

Table 4.14 ^{13}C, ^{1}H, HMBC (^{1}H-^{13}C) and COSY (^{1}H-^{1}H) correlations exhibited in the 2D NMR spectra data of 5,3′-dihydroxy-3,7,4′-trimethoxyflavone (**215**)

Position	**δ_C (DEPT)** (100 MHz in $CDCl_3$)	**δ_H (*mult, J* Hz)** (400 MHz in $CDCl_3$)	**HMBC**	**COSY**
1	-	-	-	-
2	155.67 (C)	-	-	-
3	139.14 (C)	-	-	-
4	178.82 (C=O)	-	-	-
5	161.96 (C)	-	-	-
6	97.87 (CH)	6.38 (*d*, 2.2)	C-5, C-7, C-8, C-10	H-8
7	165.44 (C)	-	-	-
8	92.12 (CH)	6.47 (*d*, 2.2)	C-6, C-7, C-9, C-10	H-6
9	156.74 (C)	-	-	-
10	106.10 (C)	-	-	-
1′	123.62 (C)	-	-	-
2′	114.39 (CH)	7.72 (*d*, 2.2)	C-2, C-3′, C-4′, C-6′	-
3′	145.50 (C)	-	-	-
4′	148.63 (C)	-	-	-
5′	110.36 (CH)	6.99 (*d*, 8.6)	C-1′, C-3′	H-6′
6′	121.58 (CH)	7.75 (*dd*, 8.6, 2.2)	C-2′, C-4′	H-5′
3-OCH_3	60.16 (CH_3)	3.89 (*s*)	C-3	-
7-OCH_3	55.80 (CH_3)	3.90 (*s*)	C-7	-
3′-OH	-	5.76 (*s*)	C-2′, C-3′, C-4′	-
4′-OCH_3	56.05 (CH_3)	4.01 (*s*)	C-4′	-
5-OH	-	12.66 (*s*)	C-5, C-6, C-10	-

Remark: δ in ppm from TMS

In the present study by EIMS analysis of compound **215** ($[M]^+$, *m/z* 344) revealed that the base peak was showed at *m/z* 342 $[M-2H]^+$. The main fragments produced by the retro Diels-Alder cleavage of ring C bonds afforded the fragment ions at *m/z* 166 and *m/z* 178, respectively. The fragment occurred by the loss of methyl group $[M-CH_3]^+$, followed by the loss of dehydration $[M-CH_3-H_2O]^+$ and carbonyl group $[M-CH_3-H_2O-CO]^+$, respectively. The weak intensity of another fragment was obtained at *m/z* 151 and *m/z* 193. The fragmentation patterns of compound 215 are closely similar to flavone compounds which reported by Tsimogiannis *et al*. [134], as shown in Figure 4.15.

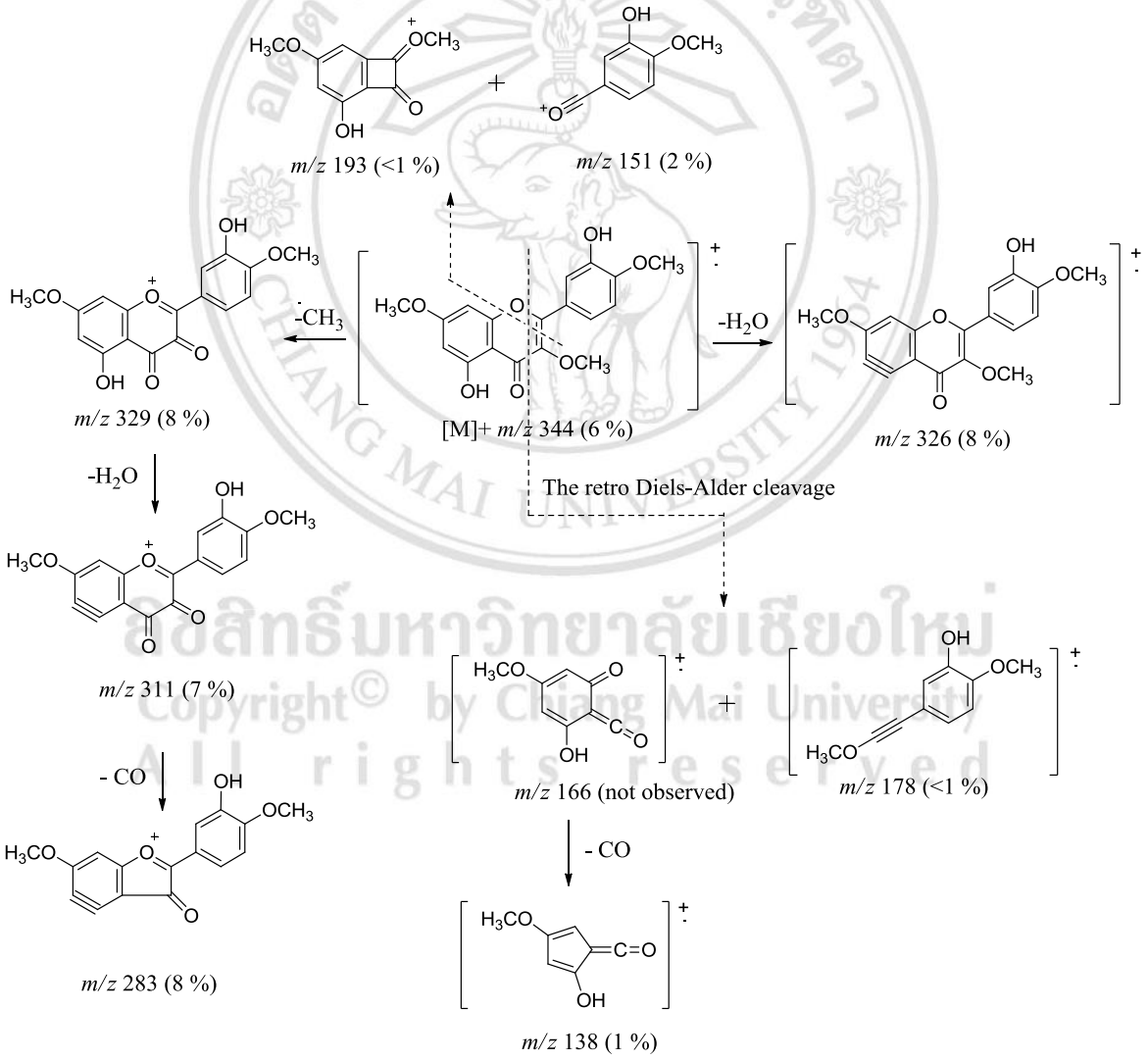

Figure 4.15 The mass spectral fragmentation patterns of 5,3′-dihydroxy-3,7,4′-trimethoxyflavone (**215**)

3) 5,3′,4′-Trihydroxy-3,7-dimethoxyflavone (**216**)

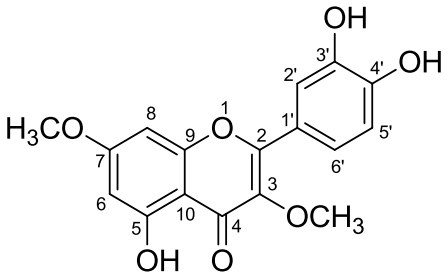

Figure 4.16 The structure of 5,3′,4′-trihydroxy-3,7-dimethoxyflavone (**216**)

Compound **216** was isolated as yellow needles which recrystallized with mixture of 95% EtOH and acetone, mp 242.8–243.2 ºC (Lit. 242.0–243.0 ºC [137]). The other names was 3,7-*O*-trimethylquercetin. The EI mass spectrum gave a molecular ion peak at m/z 330 $[M]^+$, corresponding to the molecular formula $C_{17}H_{14}O_7$. The UV absorptions maximum at λ_{max} 355, 257 and 208 nm in MeOH. The IR spectrum revealed the absorption bands at 3450 and 1660 cm^{-1} attributed to the existence of hydroxyl and carbonyl group in this structure. The C=C stretching bands of aromatic system were assigned at 1600, 1500 and 1440 cm^{-1}.

The ^1H NMR spectrum (Table 4.15) showed the presence of *meta*-coupled protons at δ 6.33 (*d*, *J* = 2.2 Hz, H-6) and δ 6.67 (*d*, *J* = 2.2 Hz, H-8) of ring A. The three aromatic protons of ring B were assigned at δ 7.74 (*d*, *J* = 2.1, H-2'), 7.02 (*d*, *J* = 8.5 Hz, H-5') and 7.62 (*dd*, *J* = 8.5, 2.1 Hz, H-6'). The spectrum revealed the presence of two methoxyl groups at δ 3.89 (*s*, 3-OCH_3), 3.94 (*s*, 7-OCH_3), respectively. This structure was confirmed by the presence of a chelated hydroxyl proton at δ 12.79 (*s*) for 5-OH position. While, two hydroxyl protons at position 3'-OH and 4'-OH not showed spectrum for compound **216** due to the phenolic compounds are easily labile.

The ^{13}C NMR and DEPT spectra showed the presence of 17 carbons, including one carbonyl carbon, nine quarternary carbons, five methine carbons and two methoxyl carbons as shown in Table 4.15.

By comparing its ^1H and ^{13}C NMR data with literature data [137]

(Table 4.15), and confirmed structure by 2D NMR techniques (Table 4.16), this compound was considered as 5,3′,4′-trihydroxy-3,7-dimethoxyflavone.

Table 4.15 ^{1}H and ^{13}C NMR data of 5,3′,4′-trihydroxy-3,7-dimethoxyflavone (**216**) in comparison with the previously reported [137]

Position	Compound 216		Ref. [137]	
	δ_H (*mult, J* Hz) (400 MHz in $CDCl_3$)	δ_C (DEPT) (100 MHz in $CDCl_3$)	δ_H (*mult, J* Hz) (270 MHz in DMSO-d_6)	δ_C (DEPT) (67.8 MHz in DMSO-d_6)
1	-	-	-	-
2	-	156.06 (C)	-	155.9 (C)
3	-	138.54 (C)	-	137.8 (C)
4	-	178.68 (C=O)	-	177.9 (C=O)
5	-	161.93 (C)	-	156.2 (C)
6	6.33 (*d*, 2.2)	97.55 (CH)	6.37 (*d*, 2.0)	97.6 (CH)
7	-	165.65 (C)	-	165.0 (C)
8	6.67 (*d*, 2.2)	91.87 (CH)	6.71 (*d*, 2.0)	92.1 (CH)
9	-	156.81 (C)	-	160.9 (C)
10	-	105.64 (C)	-	105.1 (C)
1′	-	122.09 (C)	-	120.6 (C)
2′	7.74 (*d*, 2.1)	115.49 (CH)	7.59 (*d*, 2.0)	115.4 (CH)
3′	-	144.98 (C)	-	145.3 (C)
4′	-	148.26 (C)	-	149.0 (C)
5′	7.02 (*d*, 8.5)	115.35 (CH)	6.91 (*d*, 8.0)	115.6 (CH)
6′	7.62 (*dd*, 8.5, 2.1)	121.27 (CH)	7.49 (*dd*, 8.0, 2.0)	120.4 (CH)
3-OCH_3	3.89 (*s*)	59.26 (CH_3)	3.86 (*s*)	59.6 (CH_3)
7-OCH_3	3.94 (*s*)	55.52 (CH_3)	3.80 (*s*)	56.0 (CH_3)
3′-OH	-	-	-	-
4′-OH	-	-	-	-
5-OH	12.79 (*s*)	-	-	-

Remark: δ in ppm from TMS

Table 4.16 ^{13}C, ^{1}H, HMBC (^{1}H-^{13}C) and COSY (^{1}H-^{1}H) correlations exhibited in the 2D NMR spectra data of 5,3′,4′-trihydroxy-3,7-dimethoxyflavone (**216**)

Position	**δ_C (DEPT)** (100 MHz in $CDCl_3$)	**δ_H (*mult, J* Hz)** (400 MHz in $CDCl_3$)	**HMBC**	**COSY**
1	-	-	-	-
2	156.06 (C)	-	-	-
3	138.54 (C)	-	-	-
4	178.68 (C=O)	-	-	-
5	161.93 (C)	-	-	-
6	97.55 (CH)	6.33 (*d*, 2.2)	C-5, C-7, C-8, C-10	H-8
7	165.65 (C)	-	-	-
8	91.87 (CH)	6.67 (*d*, 2.2)	C-6, C-7, C-9, C-10	H-6
9	156.81 (C)	-	-	-
10	105.64 (C)	-	-	-
1′	122.09 (C)	-	-	-
2′	115.49 (CH)	7.74 (*d*, 2.1)	C-2, C-3′, C-4′, C-6′	-
3′	144.98 (C)	-	-	-
4′	148.26 (C)	-	-	-
5′	115.35 (CH)	7.02 (*d*, 8.5)	C-1′, C-3′, C-4′	H-6′
6′	121.27 (CH)	7.62 (*dd*, 8.5, 2.1)	C-2, C-2′, C-4′, C-5′	H-5′
3-OCH_3	59.26 (CH_3)	3.89 (*s*)	C-3	-
7-OCH_3	55.52 (CH_3)	3.94 (*s*)	C-7	-
3′-OH	-	-	-	-
4′-OH	-	-	-	-
5-OH	-	12.79 (*s*)	C-5, C-6, C-7, C-10	-

Remark: δ in ppm from TMS

The EIMS analysis of compound **216** ($[M]^+$, *m/z* 330) exhibited the base peak at *m/z* 328 $[M-2H]^+$. The main fragmentation was produced by the retro Diels-Alder cleavage of ring C bonds obtained the fragment ions at *m/z* 166 and *m/z* 164. The another fragment appeared by the loss of methyl group $[M-CH_3]^+$, followed by the loss of dehydration $[M-CH_3-H_2O]^+$ and carbonyl group $[M-CH_3-H_2O-CO]^+$, respectively. The fragment ions at *m/z* 137 and *m/z* 193 indicated that the minor fragment pattern, which have also been observed by Tsimogiannis *et al*. [134], as shown in Figure 4.17.

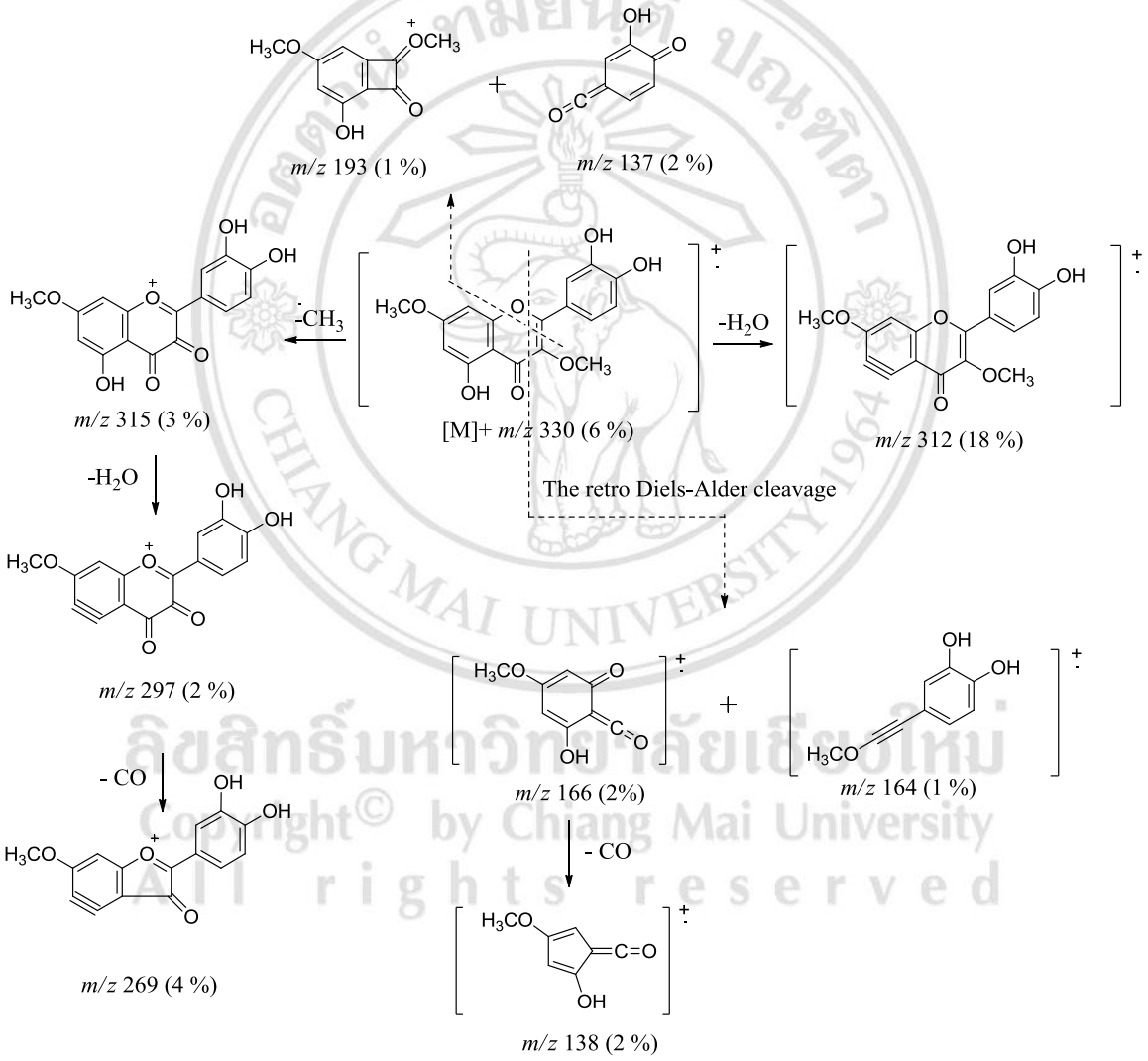

Figure 4.17 The mass spectral fragmentation patterns of 5,3′,4′-trihydroxy-3,7-dimethoxyflavone (**216**)

Due to three flavones **214**, **215** and **216** are a class of flavonoids, a group of plant polyphenolic secondary metabolites, so these compounds are synthesized through the phenylpropanoids pathway, transforming phenylalanine into 4-coumaroyl-CoA, which finally enters the flavonoids biosynthesis pathway [138].

4.2.2 Biological Activity of *P. bullata*

In the preliminary investigations of crude extract from *P. bullata*, the cytotoxic testing was evaluated by our collaborator from Faculty of Science, Mahidol University. The cytotoxicity were recorded as ED_{50} values below 20 μg/mL against on P-388, KB, HT29, MCF-7, A549, ASK and HEK-293 cell lines. The result showed that the hexane extract against on ASK and HEK-293 cell lines with ED_{50} values of 19.46 and 1.84 μg/mL, respectively. The ethyl acetate was inhibited on P-388 and MCF-7 cell lines with ED_{50} values of 6.05 and 19.28 μg/mL, respectively, while the methanol extract no ED_{50} values below 20 μg/mL on all cell lines.

Table 4.17 Cytotoxic activities of the extracts from the aerial parts of *P. bullata*

Extract	ED_{50} (μg/mL)						
	P-388	**KB**	**HT29**	**MCF-7**	**A549**	**ASK**	**HEK-293**
Hexane	>20	>20	>20	>20	>20	19.46	1.84
EtOAc	6.05	>20	>20	19.28	>20	>20	>20
MeOH	>20	>20	>20	>20	>20	>20	>20
Ellipticine	0.43	0.45	0.64	0.51	0.48	0.59	0.45

ED_{50} <20 μg/mL is considered active
P-388: murine lymphocytic leukemia, KB: human oral epidermoid carcinoma, HT29: human colon carcinoma, MCF-7: human breast cancer, A549: adenocarcinomic human alveolar basal epithelial cells, ASK: rat glioma cell, HEK-293: human embryonic kidney.

Further, all crude extracts were isolated and purified to yield three compounds (**214**–**216**). The compounds were evaluated cytotoxicity and selectivity on six cancer cell lines (P-388, KB, HT29, MCF-7, A549, ASK) and one normal cell line (HEK-293). The most active compound was compound **216** which exhibited high active on P-388 (ED_{50} 7.13 μg/mL) but less selectivity (SI=2.8) and moderate active on MCF-7 cell lines (ED_{50} 18.16 μg/mL) but less selectivity (SI=1.1), but compound **214** and **215** were inactive on all cell lines (ED_{50} >20 μg/mL) and no selectivity. These results are in

agreement with the preliminary cytotoxic of crude extracts (Table 4.17). Interestingly, compound **216** was higher selectivity (SI=2.8) to P-388 cell line than ellipticine (SI=1.3), which used as positive control. Whereas, compound **216** showed lower selectivity (SI=1.1) to MCF-7 cell line than ellipticine (SI=1.3). Therefore, indicating that compound **216** has good selectivity to P-388 cell line for cytotoxic tested. The results of cytotoxic activity were shown in Table 4.18.

Table 4.18 Cytotoxic activities of the isolated compounds from the aerial parts of *P. bullata*

Compound	ED_{50} (μg/mL)						
	P-388	**KB**	**HT29**	**MCF-7**	**A549**	**ASK**	**HEK-293**
214	>20	>20	>20	>20	>20	>20	>20
215	>20	>20	>20	>20	>20	>20	>20
216	7.13	>20	>20	18.16	>20	>20	>20
Ellipticine	0.46	0.58	0.66	0.50	0.62	0.66	0.59

ED_{50} <20 μg/mL is considered active
P-388: murine lymphocytic leukemia, KB: human oral epidermoid carcinoma, HT29: human colon carcinoma, MCF-7: human breast cancer, A549: adenocarcinomic human alveolar basal epithelial cells, ASK: rat glioma cell, HEK-293: human embryonic kidney.

By comparing the cytotoxicity of three flavones **214**–**216**, there were reported several structure-activity relationships (SAR) associated with increased cytotoxicity on cancer cell lines, including the presence of a C2-C3 double bond, a C4-carbonyl group, *ortho*-hydroxylation in B ring, C7-methoxy substitution in A ring, C3-methoxy substitution in C ring and C3′, C4′-dihydroxylation [139-141]. Because the flavones **214**–**216** are similarly structures except at C3′ and C4′ substitutions, so the substitutions of these positions seem to be associated with enhanced cytotoxicity for cancer cell lines as well. Apparently, the presence of C3′, C4′-dihydroxyflavone of compound **216** led to a significant increase in cytotoxicity on P-388 and MCF-7 cell lines more than another compounds, which agreement with previous study that has also identified the importance of these positions for cytotoxicity [141].

Previously, compounds **214**–**216** were investigated for their cytotoxicities on many cancer cell lines such as, compound **214** showed selective

activities with IC_{50} values below 30 μg/mL against drug-sensitive leukemia CCRF-CEM (18.38 μg/mL), multidrug-resistant P-glycoprotein over-expressing leukemia CEM/ADR5000 (18.22 μg/mL) [142], MCF-7 (46.59 μg/mL) and oral squamous carcinoma BHY (46.04 μg/mL) cell lines [143]. Compound **215** exhibited cytotoxic against human leukemia HL-60 cell line with IC_{50} values at 55 μg/mL [144]. Whereas, compound **216** has not been showed cytotoxicities.